Corrugated surface plasmon resonance optical transducer

E.P. Rodrigues[a], A.M.N. Lima[a], H. Neff[a]
[a]UFCG/CEEI/PPgEE
Campina Grande, PB, Brazil
[eloise.rodrigues,amnlima]@ee.edu.br,heneff@web.de

L.C. Oliveira[a,b], T.A.T. Sousa[a,c]
[b]UFERSA, [c]IFAL
[b]Angicos-RN, [c]Palmeira dos Indios-AL
[leiva.oliveira;tiago.sousa]@ee.ufcg.edu.br

ABSTRACT

This paper presents theoretical and experimental results of a periodic grating surface plasmon resonance (SPR) transducer. The angular interrogation mode, for a fixed wavelength of 820 nm, was explored at specular reflection for gold films, deposited by sputtering on a grooved polymer substrate. The thin metal layer has a height of 50 nm and a pitch of 478 nm. Parameters such as resonant angle and sensitivity have been determined. Coherence between the theoretical and experimental results demonstrates the correctness of the proposed methodology and the feasibility of the proposed device.

KEYWORDS

SPR, grating, transducer, sensor

ACM Reference format:
E.P. Rodrigues[a], A.M.N. Lima[a], H. Neff[a] and L.C. Oliveira[a, b], T.A.T. Sousa[a, c]. 2017. Corrugated surface plasmon resonance optical transducer. In *Proceedings of 17th Microelectronics Students Forum, Fortaleza-CE, Brazil, July 2017 (SFORUM'17),* 4 pages.
https://doi.org/10.1145/nnnnnnn.nnnnnnn

1 INTRODUCTION

The surface plasmon resonance (SPR) phenomenon has been extensively studied in the last years and has its applications mainly directed to the construction of optical sensors. SPR sensors are quite versatile and widely used in optical instruments for real-time monitoring of biochemical interactions in an aqueous environment [1, 10]. The excitation of plasmons is mainly based on the Otto and Kretchsmann configurations, however, its analysis may be modified due to changes in the shape of the metal surface, which may be smooth, rough or a periodic grating.

The SPR phenomenon consists of a longitudinal oscillation in charge density, along the interface between two media with opposing signal dielectric constants, where one is metal and the other is a dielectric [4]. Coupling and resonant interaction of the surface plasmon (SP) wave with a received photon requires that the SP-wave vector k_{sp} corresponds to the incident light wave vector k_{ph}, corresponding to energy-momentum conservation.

In SPR transducers the grating can be used in two different ways, they are: direct incidence of light on the grating, which provides an incident wave vector impulse coupled to the surface due to its periodic geometry, or still indirect incidence at which light is guided through a prism by using the attenuated total reflection (ATR) technique [2]. To augment k_{ph} under conditions where the incident light beam propagates through vacuum or gas, with $n \approx 1$, the reflective surface must be spatially modulated through a corrugated surface profile, to establish appropriate momentum transfer. The former condition is denoted the grating mode (GM).

In this work a sensor system is designed in which the incident light (820 nm) is applied directly on the metallic grating surface. To determine the sensor response, numerical simulations are performed, and a laboratory test set-up was built. The GM mode was used under specular reflection conditions for variation of the angle of incidence (GM-AIM).

SFORUM'17, July 2017, Fortaleza-CE, Brazil

ACM ISBN 978-x-xxxx-xxxx-x/YY/MM.
https://doi.org/10.1145/nnnnnnn.nnnnnnn

1.1 Theoretical aspects

The periodic grating consists of a surface characterized by multiple slits or parallel grooves in a given substrate, which follow a periodicity (Λ). When light is shed onto the surface the light beams are reflected, absorbed or transmitted having characteristic angles for each diffraction order as illustrated in Figure 1. The grating

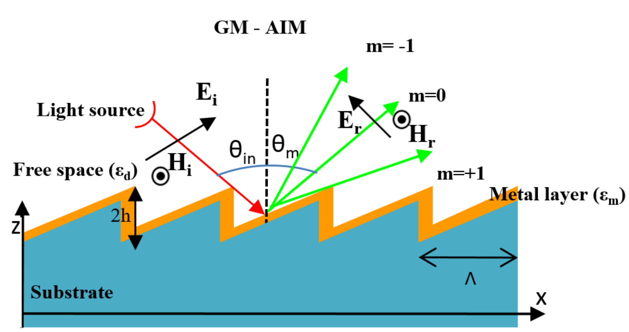

Figure 1: Geometry of the transducer grating. A thin metallic layer is sputtered onto the corrugated polymer surface. The incident light has the polarization type P, whose the electric field is parallel to grooves of the grating.

has direct influence on the x component of the incident light wave vector k_x, resulting in the addition or subtraction of the grating vector k_g, which depends only on the diffraction order, as given by [7]:

$$k_m = k_x + mk_g \quad (1)$$

where $k_x = \frac{2\pi}{\lambda}\sin(\theta_{in})$, and m denotes the diffraction order (positive or negative integers) and $k_g = 2\pi/\Lambda$ is the diffraction grating vector which is inversely proportional to the spatial period. Since the incidence of the light rays perpendicular to the periodic surface the grating equation can be expressed by [6, 7]:

$$\frac{m\lambda}{\Lambda} + \sin(\theta_{in}) = \sin(\theta_m) \tag{2}$$

For the different diffraction orders to exist which can be considered a special case called specular reflection or zero order, where $m = 0$ for all wavelengths and the grating acts as a mirror [7].

1.2 Surface plasmon resonance on the grating

Surface plasmon can be defined as a transverse magnetic (TM) polarized electromagnetic wave which propagates along the metal/dielectric interface [3], resulting from the interaction of light with the metal electrons. The SPR technique uses the spreading of the plasmon wave that is quite sensitive to changes in refractive index close to the surface. Such sensitivity is observed at the resonance condition, i.e., when the wave vector of plasmon surface (SPW) couples the vector of incident light on metallic layer [9]. At the resonance condition the propagation constant of the SPW wave is given by [5]:

$$k_{sp} = k_0\sqrt{\frac{\varepsilon_{\mathrm{mr}} n_d^2}{\varepsilon_{\mathrm{mr}} + n_d^2}} \tag{3}$$

where $\varepsilon_{\mathrm{m}} = \varepsilon_{\mathrm{mr}} + j\varepsilon_{\mathrm{mi}}$ is the permittivity of metallic layer.

The condition for the off-specular resonance angle θ_{res} in the grating mode [8] in the gas phase writes as:

$$\theta_{\mathrm{res}} = \arcsin\left(\pm\sqrt{\frac{\varepsilon_{\mathrm{mr}} + 1}{\varepsilon_{\mathrm{mr}}}} \pm \frac{m\lambda}{\Lambda}\right) \tag{4}$$

m is an integer number, whose define if the diffraction order is positive or negative, Λ is the grating pitch (see Figure 1) and $\varepsilon_{\mathrm{mr}}$ is the metal dielectric constant at the resonance wavelength. If the incident angle satisfy the condition:

$$k_m = k_{sp} \tag{5}$$

then the SPW wave was excited and consequently coupled to the optical beam resulting in the reflection of light absorption specular, in other words the resonance condition has been achieved [4, 5].

The finite element method (FEM) was used to solve the field equations involved in the wave propagation process at the interface. The basic equation to be solved is given by

$$\nabla \times \mu_r^{-1}(\nabla \times \mathbf{E}) - k_0^2\left[\varepsilon_m - \frac{j\sigma}{\omega\varepsilon_0}\right]\mathbf{E} = \mathbf{0}. \tag{6}$$

That equation was formulated for the transducer structure shown in Figure 1. In the above equation, ω represents the wave frequency, ε_{mr} is real part of permittivity of metal, ε_0 and μ_r are respectively the gold and vacuum permittivity, the permeability, σ is the conductivity, $k_0 = \frac{2\pi}{\lambda}$ and $\mathbf{E}$ is electric field vector. The boundary conditions are $\mathbf{N} \times \nabla\mathbf{E} = \mathbf{0}$ and $\mathbf{N} \times \nabla\mathbf{H} = \mathbf{0}$ [4], where $\mathbf{N}$ denotes the vector normal to the surface of the grating.

For the proposed transducer structure, the light beam has directly incidence on the metal layer. The light had polarization of type S (or TE mode) and type P (or TM mode), whose direction of the electric and magnetic fields can be seen in the Figure 2. The transducer output signal is the ratio of P/S field intensities.

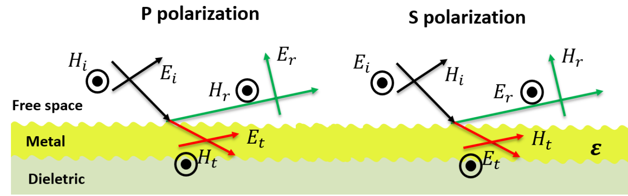

Figure 2: a) Scanning and b) Cross-sectional high resolution images of the grating's profile.

1.3 Simulations and Experiments

From a cut on the chip the transverse grooves of the grating, a microscopic analysis was performed [9] and the profile of this grating could be determined. The result of this study is presented in Figure 3, consisting of a sawtooth waveform geometry with rounded edges. For the numerical study a spatial Fourier series expansion of the actual grating surface was used.

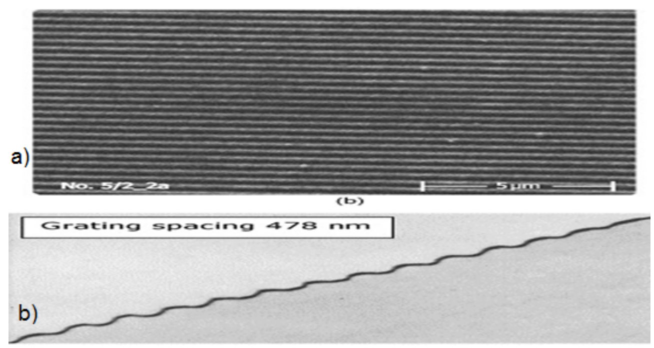

Figure 3: a) Scanning and b) Cross-sectional high resolution images of the grating's profile.

Parameter	Value
Periodicity (Λ)	478 (nm)
Height of the structure	500 (nm)
Height of the grating	100 (nm)
Height of the metallic layer	50 (nm)
IR of air	1
IR of substrate	1.52
Incident angle	θ_{in} (0-90 deg)
Wavelength	820 nm
Frequency	$3 \times 10^8/\lambda$

The computational study was performed with the help of the COMSOL software for the structure sketched in Figure 4. The parameters used in numerical study are given in Table 1. The sinusoidal waveform resulted from the use of the first harmonic obtained from Fourier series expansion, whose the periodicity is 478 nm. As the study carried out was AIM, we have a fixed wavelength of light at 820 nm, however, we have the incidence angle ranging from 10-90 deg. An optical diffraction grating, manufactured by injection molding of a cyclic olefin co-polymer (tradename TOPAS), has been exploited for this investigation. The device comprises a 50 nm gold

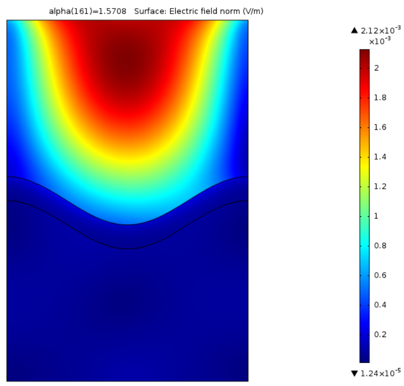

Figure 4: Numerical results for the electric field intensity near the metal-dielectric interface. The transducer is composed of TOPAS and gold (bluish area). The incident light is directed to the metallic layer. The intensity of electric field (V/m) observed at/around the air/gold interface follows the color code seen in the right hand side.

film deposited by sputtering exhibiting a pitch of 478 nm. The device has two areas provided with gratings that were coated with a layer of gold (See Figure 5). For the implementation of the proposed

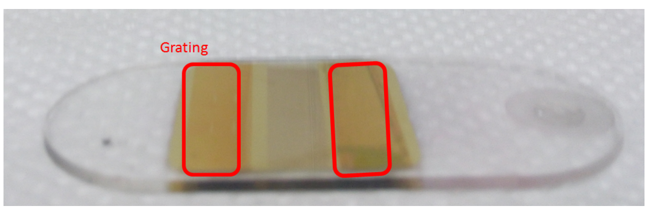

Figure 5: Transducer built for experimental tests. The device has two similar grating regions. Thus it is possible to use any one of the grooved regions.

system is used an optical assembly kit composed of lenses, light source, optical bandpass filter (820 nm) and spectrometer. The optical source used in the experiment is a stabilized tungsten-halogen light source providing a constant-intensity of 10 mW blackbody (blackbody spectrum spans both in the visible and near-infrared regions) radiation spectrum between 360 and 2600 nm. The optical filter allows part of the light beam to be discarded, thus using only the 820 nm light wave length. The lenses, polarizer and shutter, are responsible for directing the beam of light. A spectrometer is used to capture the reflected light. The assembled system is shown in Figure 6. The test set-up structure is detailed in Figure 6 and the optical set-up is shown in a photographic image in Figure 7, respectively. The spectral position of the resonance is extracted from the reflectance ratio P/S of the s- and p-polarized components. The experimental protocol is to excite the corrugated surface with a p-polarized light at a specific incident range of angles and measure the reflected beam by using the image detector. The corrugated surface is exposed to the ambient (laboratory) air.

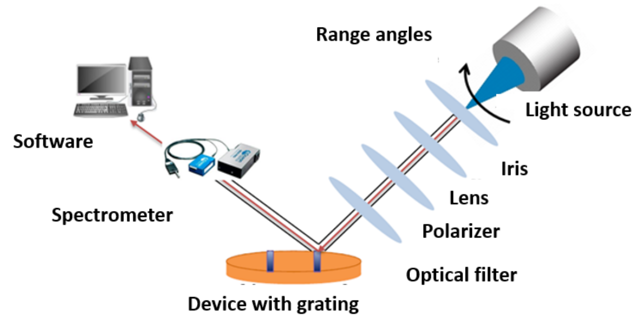

Figure 6: Detailed diagram of the experimental test setup.

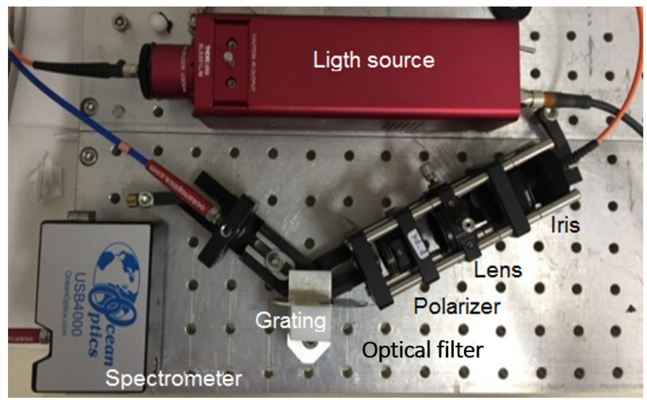

Figure 7: Photo of of experimental test setup.

The variation of the angle of incidence was performed manually and restricted to a range close to the resonance angle (the wavelength was fixed at 820 nm). A custom designed software was used to acquire and process the spectrometer data via an USB connection. Once all components are correctly positioned, the incident light is directed on the metal grating and the software is initialized to plot the SPR curves, making a pixel $\times$ θ relationship. The intensity of reflected light by the device is captured by the spectrometer for each angle of incidence. From the data obtained for each angle it is possible to trace the SPR curve in AIM mode.

2 RESULTS AND DISCUSSION

In the Figures 8 and 9, are showed the results of the simulated ans experimental curves, comprising in a ratio of fields (P/S) with different polarizations and the experimental curve obtained from a software whose function is to determine the minimum luminosity obtained through the grating. The figures exhibit grating resonance in the GM-AIM for the gold metallic grating in the order $m = 0$.

When analyzing the experimental and simulated results it is possible to verify that the resonance occurs at the same point, approximately at the 45 deg. However, it is noticeable that the simulated curve presents better behavior, free of noise and loss of reflectivity in almost 100%, whereas the experimental curve shows some fluctuations and less loss of reflectivity. The characteristics of the experimental curve can be explained by the high sensitivity of the used spectrometer associated with other factors such as the luminosity of the environment that can not be ruled out. Associated with this set of factors we also have that the simulated surface consisted of a perfectly deposited metallic grating profile, however, it is not possible to say that this occurred in practice.

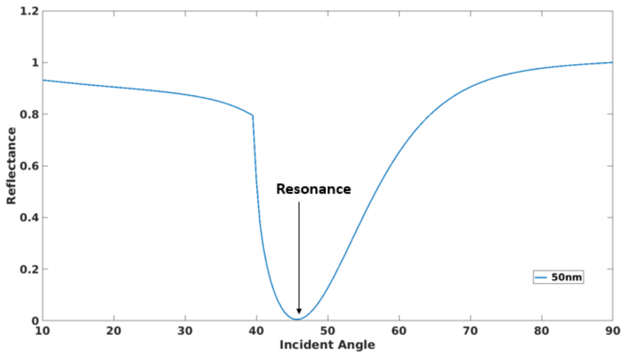

Figure 8: Simulated SPR curve obtained for a grating of 478 nm and incident light beam with wavelength 820 nm. As expected, the curve shows a drop in the reflectivity of almost 100% in the region comprising the angles close to 45 deg.

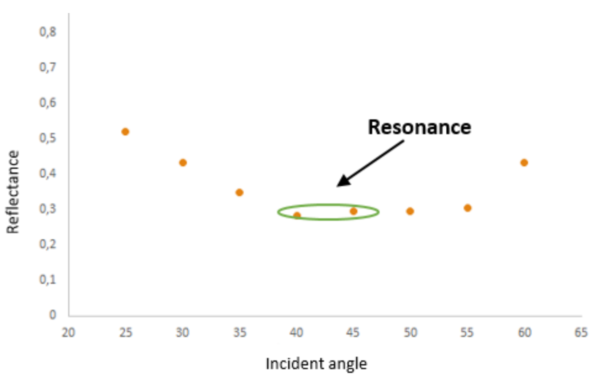

Figure 9: Experimental SPR curve, in the AIM mode, obtained with the test setup for a incident light beam with wavelength 820 nm and incident angle range of 20-90 deg. The curve shows a drop in the reflectivity of almost 80% in the region comprising the angles close to 40-45 deg.

The sensitivity of the transducer in the metal grating is theoretically determined by artificially varying the refractive index of the air from 1 to 1.05. Figure 10 shows the changes in the resonance curve to change the refractive index, so it is possible to calculate the sensitivity from (7)

$$S_{\mathrm{AIM}}^{\mathrm{GM}} = \frac{\Delta\theta}{\Delta n} \tag{7}$$

Thus, following the displacement of the SPR curve for a change of 0.05 in the refractive index unit (RIU), it is correct to state that the SPR sensor system based on the diffraction grating had a calculated sensitivity of approximately 80 deg/RIU.

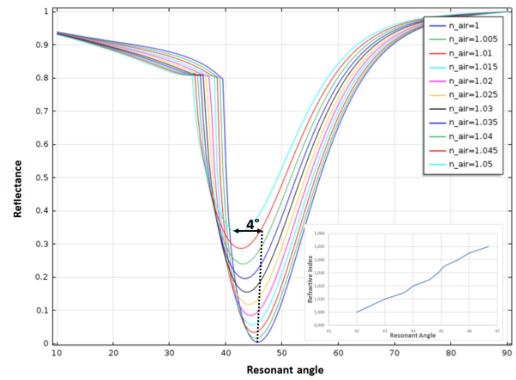

Figure 10: Influence of the refractive index on the SPR curve for the simulated grating. For a change of 0.5 in steps of 0.05 the SPR curve undergoes changes in both the reflectance deep and the resonance angle.

3 CONCLUSION

This article presented the characterization of a transducer based on the periodic grating used in a SPR sensor system. For the direct incidence of the light beam, simulated and experimental results present a resonance curve restricted to a similar angular range of approximately 45 deg. Despite the adopted conditions of a smoothed profile for the simulation and fluctuations in the experimental curve, it is possible to affirm that the answers agree on the result. Sensitivity test was calculated in the GM-AIM mode showing a variation of 80 deg/ RIU, showing the efficiency of the sensor system.

REFERENCES

[1] A Abbas, MJ Linman, and Q Cheng. 2011. New trends in instrumental design for surface plasmon resonance-based biosensors. *Biosensors and Bioelectronics* 26, 5 (2011), 1815–1824.
[2] CJ Alleyne, AG Kirk, RC McPhedran, N-AP Nicorovici, and D Maystre. 2007. Enhanced SPR sensitivity using periodic metallic structures. *Optics express* 15, 13 (2007), 8163–8169.
[3] J Dostalek and J Homola. 2008. Surface plasmon resonance sensor based on an array of diffraction gratings for highly parallelized observation of biomolecular interactions. *Sensors and Actuators B: Chemical* 129, 1 (2008), 303–310.
[4] E Fontana. 2004. Theoretical and experimental study of the surface plasmon resonance effect on a recordable compact disk. *Applied optics* 43, 1 (2004), 79–87.
[5] J Homola, I Koudela, and SS Yee. 1999. Surface plasmon resonance sensors based on diffraction gratings and prism couplers: sensitivity comparison. *Sensors and Actuators B: Chemical* 54, 1 (1999), 16–24.
[6] C A Palmer and EG Loewen. 2005. *Diffraction grating handbook.* Newport Corporation, Rochester, USA.
[7] E Popov. 2012. *Gratings: theory and numeric applications.* Institut Fresnel, Marseille, FR.
[8] H Raether. 1988. *Surface plasmons on smooth surfaces.* Springer, Heidelberg, DE.
[9] C Thirstrup, W Zong, M Borre, H Neff, HC Pedersen, and G Holzhueter. 2004. Diffractive optical coupling element for surface plasmon resonance sensors. *Sensors and Actuators B: Chemical* 100, 3 (2004), 298–308.
[10] L Tong, H Wei, S Zhang, and H Xu. 2014. Recent advances in plasmonic sensors. *Sensors* 14, 5 (2014), 7959–7973.